Measuring the Unusually Slow Ionic Diffusion in Polyaniline via Study of Yolk-Shell Nanostructures

Hang Sun,[†] Xiaoshuang Shen,[†] Lin Yao,[†] Shuangxi Xing,[‡] Hong Wang,[†] Yuhua Feng,[†] and Hongyu Chen*,[†]

[†]Division of Chemistry and Biological Chemistry, Nanyang Technological University, Singapore 637371
[‡]Faculty of Chemistry, Northeast Normal University, Changchun 130024, China

Ⓢ *Supporting Information*

ABSTRACT: We demonstrate a unique capability in partially oxidizing the oligoaniline shell on gold nanoparticles to polyaniline. Because of the solubility difference, the unreacted inner shell section can be selectively dissolved by 2-propanol, giving yolk-shell nanostructures and, thus, making it possible for assessing the oxidized section. The ionic diffusion through the polymer shell is found to be the rate-determining step in the overall process. Conservative estimates show that the diffusion coefficient of $AuCl_4^-$ is at least 700 times slower than that of the typical rate values in traditional studies. It is most likely caused by the lack of micropores in the polymer structures. Such mircopores are hard to avoid in preparing polymer membranes by casting or drying of polymers dissolved in organic solvents. We can rule out the presence of irregular pores on the basis of the uniformly oxidized shell section. With the nanoscale shells, the system is sensitive enough to detect minute changes in the shell or small differences among the individual nanoparticles. Even with a small increase in porosity, for example, when the polyaniline shell is swollen using small amounts of DMF (3%, 5%, or 10% in aqueous solutions), the diffusion coefficient of $AuCl_4^-$ increases to 4, 11, and 17 times, respectively. Thus, our study demonstrates a new methodology for studying the diffusion of ions in hydrophobic polymers.
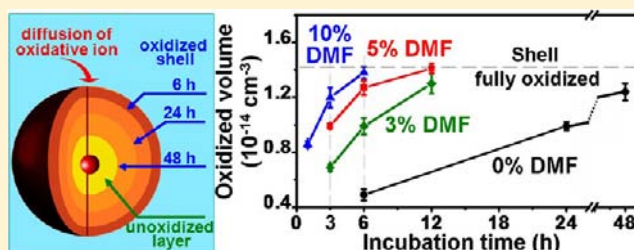
INTRODUCTION

Controlling and understanding the diffusion of ions in polymer are of great importance for applications, such as fuel cells, sensors, and reverse osmosis.[1–5] Traditionally, study of permeability in polymer was often carried out using membranes, where it is difficult to evaluate the contributions resulting from micro- and mesopores. It is well-known that porosity in polymer can facilitate the diffusion of ions.[3,4] In general, it is easier to reduce pore formation and achieve uniform polymer growth in nanostructures than in large membranes. However, there is a lack of means for evaluating ionic diffusion through nanoscale polymer structures. In order to do so, the effects of the ionic diffusion (e.g., oxidation or etching) must be measurable and most importantly, the diffusion has to be the rate-determining step in the overall process.

Yolk-shell structure is a special type of hollow structure, which has attracted much interest for its potential usage in chemical storage and compartmentalization.[6] It contains a core inside a void space surrounded by a shell.[7,8] As such, the shell protects the core while acting as a permeable barrier; the void could retain chemicals for interacting with the core. Recent studies have demonstrated that the combination of core, hollow space, and permeable shell could give rise to improved properties in catalysis,[9–11] energy storage,[12,13] and drug delivery.[14] Typical synthesis of yolk-shell nanoparticles (NPs)

involves the etching of a sacrificial layer. Thus, the method often requires triple-layered structures, which are synthetically challenging considering the multistep growth and selective etching.[7,10,11,15] An alternative method is to partially etch the outer section of the core[9,16] or the inner section of the shell. While this approach only requires double-layered structure, it is a challenge to control the partial etching process and obtain uniform products.

Several methods have been reported on the partial hollowing of metal and oxide shells: During the galvanic replacement of a metal shell,[17] the faster outward diffusion of the shell material than the inward diffusion of the new deposition layer leads to a net inflow of vacancies, which condense into a void space (the Kirkendall effect).[18] On the other hand, oxide shells (mostly silica) can be partially etched by exploiting (a) the surface regrowth of the dissolved inner layer,[19] (b) the protection of outermost layer by polyvinylpyrrolidone (PVP),[20] or (c) the inhomogeneity present in the shells.[21,22] However, partial selective etching of organic/polymer shell has so far not been demonstrated, although polymer has been widely used as building material in nanostructure synthesis.[23–25]

Here, we report a unique system where the diffusion of oxidative ions in polymer is slower than the concomitant
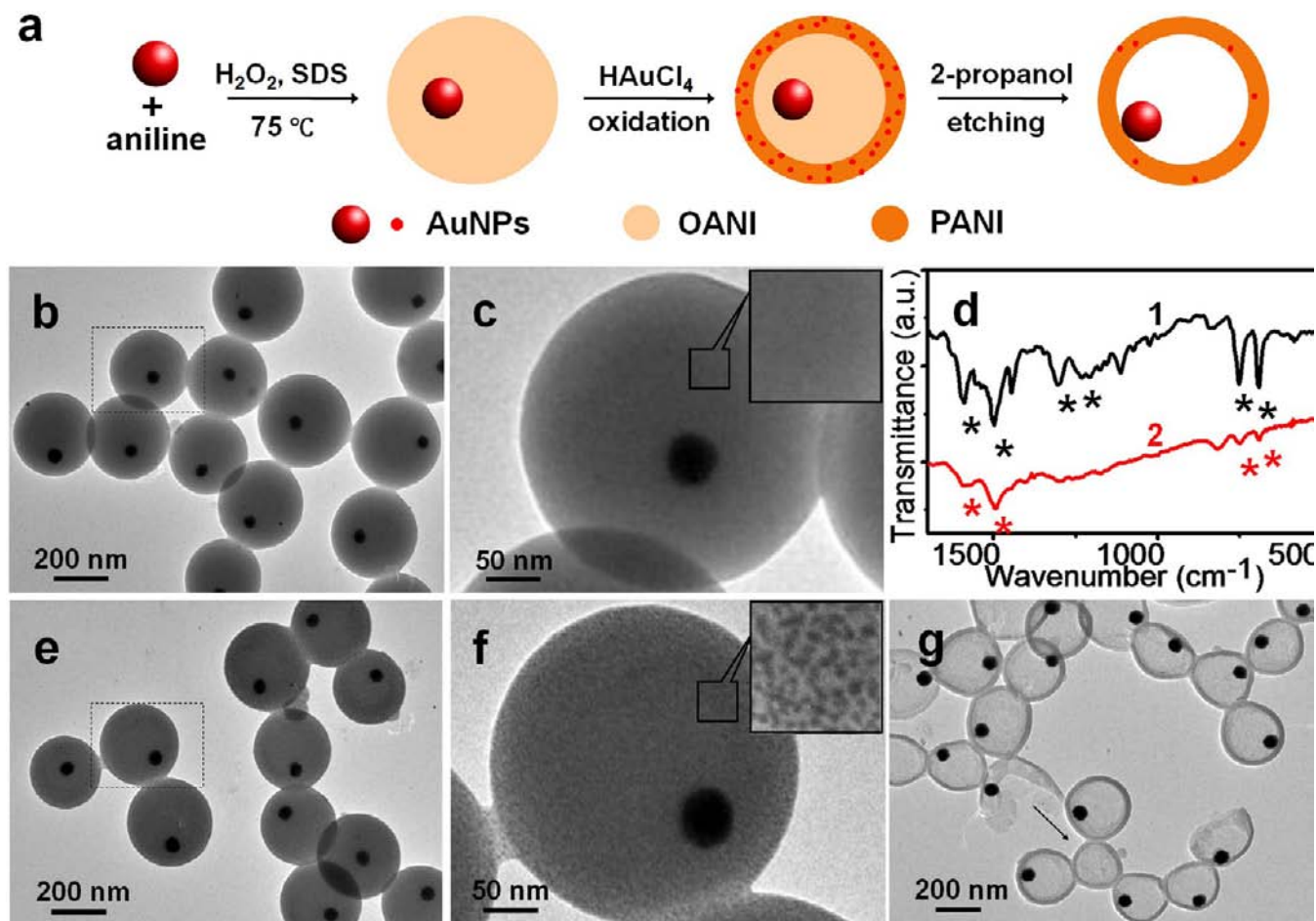
Figure 1. (a) Schematics illustrating the fabrication of Au@PANI yolk-shell NPs. TEM images of (b,c) Au@OANI core−shell NPs at low and high magnification, respectively. (d) IR spectra of (1) Au@OANI and (2) Au@PANI NPs (asterisks indicate peaks of interest). (e,f) After treating sample (b) with HAuCl$_4$ for 6 h, imaged at low and high magnification, respectively; and (g) after etching sample (e) with 2-propanol for 2 h. The arrow indicates a hollow PANI shell formed in the absence of Au core.

oxidation, making the former the rate-determining step. This simple and yet controllable process allows the evaluation of ionic diffusion rate in addition to dexterity in synthetic design. When an oligoaniline (OANI) shell on AuNPs is partially oxidized to polyaniline (PANI), the decrease in solubility allows the unreacted shell section to be easily dissolved away using 2-propanol, leading to uniform yolk-shell nanostructures (Figure 1) where the extent of oxidation can be evaluated. We find the diffusion of HAuCl$_4$ in the OANI/PANI shells to be extremely slow. Even with conservative estimates, it is at least 700 times slower than the literature values. This could be attributed to the lack of pores in these nanoscale shells.

⬛ RESULTS AND DISCUSSION

Preparation of Yolk-Shell Nanostructures. The overall process is illustrated in Figure 1a. Au@OANI core−shell NPs were prepared by in situ polymerization of aniline[26,27] on the surface of AuNPs with the help of surfactant SDS; the method was modified from our previous synthesis of Au@PANI NPs.[28] Specifically, citrate-stabilized AuNPs (40 nm) were mixed with aniline (81.2 mM) and SDS (2.5 mM), followed by addition of 81.2 mM H$_2$O$_2$ as oxidant. After 12 h incubation at 75 °C, the solution turned from the red color of AuNPs to brown, indicating aniline polymerization.[26] The resulting Au@OANI core−shell NPs were isolated by centrifugation and then

dispersed in an aqueous solution of HAuCl$_4$ (10 mM, 0.5 mL) for a specified time (6−48 h) to partially oxidize their shells. The NPs were isolated from the excess HAuCl$_4$ by centrifugation and incubated in 2-propanol for 2 h to dissolve away the unreacted inner shell section. The final product can be redispersed in water and remain stable. It was collected by centrifugation and then characterized.

Figure 1b,c shows the transmission electron microscopy (TEM) images of the Au@OANI core−shell NPs with a uniform diameter of about 300 nm. The shells were probably made of OANI of short length: It is known in the literature that short OANI is favored when the polymerization occurs either at neutral pH[26] or high temperature[29] or when a weak oxidant, such as H$_2$O$_2$, is used.[27] In our system, all three conditions were used in combination to achieve postsynthetic oxidation. Infrared (IR) spectrum of the purified Au@OANI core−shell NPs showed peaks at 1589, 1498, 1303, and 1230 cm^{-1}, confirming the polymerization of aniline (Figure 1d, line 1).[30] The additional strong bands at 752 and 692 cm^{-1} are characteristic of monosubstituted aromatic rings[29] that should occur at the terminuses of the polymer chains. Their strong intensity indicates a large population of short-chain OANI, consistent with our expectation. For convenience, we refer to both OANI and PANI as "polymer" in the following discussion. Raman spectrum of the purified Au@OANI NPs showed the

characteristic peaks at 1590, 1491, 1332, and 1170 cm⁻¹, further supporting the formation of OANI.[28,31] The molecular weight of OANI was characterized by gel permeation chromatography (GPC). The as-prepared core–shell NPs were dissolved in tetrahydrofuran (THF) and centrifuged to remove the AuNPs before measurement. The weight averaged molecular weight (M_w) was 480, which was consistent with measurements by matrix-assisted laser desorption ionization time-of-flight mass spectrometry (MALDI-ToF-MS).[31]

After being treated by HAuCl₄, the overall size of the core–shell NPs did not change, but many small AuNPs (~5 nm) can be observed on their surface (Figure 1e,f). The reduction of HAuCl₄ to Au⁰ is likely associated with the oxidation of OANI to PANI (vide infra).[32] The subsequent incubation in 2-propanol dissolved away part of the shell, leaving only a thin outer layer (Figure 1g). The clear contrast of this remaining shell with the inner void indicated the loss of the inner shell section. In magnified TEM image,[31] it was observed that the small AuNPs were also lost after this step. We were not able to characterize the oxidized polymer by GPC because it was not completely soluble in 2-propanol or THF (vide infra). Because the outer boundary of the polymer spheres did not change, we can rule out the possibility that the remaining shell was formed by the redeposition of the dissolved inner section.[19] It was apparent that the decrease in polymer solubility allowed the selective dissolution.

Hence, we have developed a facile approach to partially oxidize and then selectively etch an organic/polymer shell. The process was controllable and yielded a uniform layer of oxidized polymer with decreased solubility (the "hardened" layer). This made it possible to recognize and evaluate the oxidized section. The outer diameter of the Au@PANI yolk-shell NPs remained unchanged as that of the Au@OANI NPs, and thus, it could be tuned in the initial synthesis by adjusting the molar ratio of aniline to AuNPs. Less aniline led to thinner OANI shells (d_{av} = 110 nm); after partial oxidation and selective dissolving, Au@PANI yolk-shell NPs were obtained with smaller size and void space (Figure 2a). Different seeds, such as gold nanorods (AuNRs), could also be easily incorporated in the OANI shell and gave corresponding yolk-shell NPs (Figure 2b).
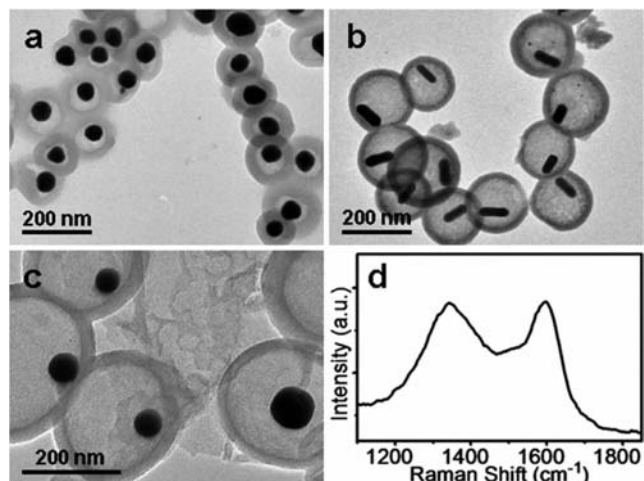

Figure 2. TEM images of (a) Au@PANI yolk-shell NPs with a small size and void space, (b) AuNR@PANI yolk-shell NPs with Au nanorods as the cores, and (c) Au@C yolk-shell NPs obtained by carbonizing Au@PANI NPs. (d) Raman spectrum of sample (c).

Importantly, the OANI/PANI shell can be converted to graphitic carbon by calcinating the Au@PANI yolk-shell NPs at 1000 °C under Ar flow. After carbonization, the resulting Au@C NPs retained the yolk-shell structure without significant structural change (Figure 2c). Figure 2d shows their Raman spectrum. There are two prominent peaks at 1597 and 1341 cm⁻¹, corresponding to the well documented G and D bands of carbon, respectively.[33,34] Their similar intensity indicated that the nanocapsule consists of semicrystalline graphitic carbon.[35]

Effects of the Shell on the Diffusion of Oxidative Ions. Because the diffusion of HAuCl₄ in the OANI/PANI shells is critical for the synthetic design, we carried out the following study to further understand the process. The rate of diffusion appeared to be much slower than those reported in the literature, as HAuCl₄ was able to penetrate only 20 nm into the OANI/PANI shell after 6 h.

A key issue in the partial oxidation of the shell is whether it was caused by inadequacy of the oxidant. When the same batch of the Au@OANI NPs was treated for a longer time (24 h) with a same concentration of HAuCl₄, the final yolk-shell nanostructures after etching showed a thicker shell (50 nm, Figure 3a). When the time was increased to 48 h, the final shells
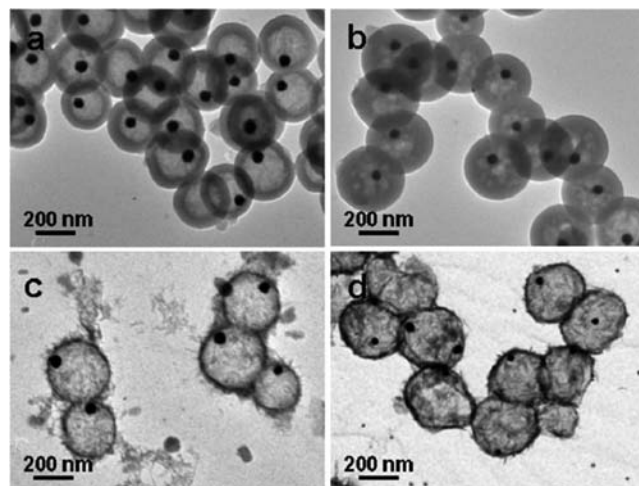

Figure 3. TEM images of the Au@PANI yolk-shell NPs that were obtained by using different oxidants and conditions: (a) 10 mM HAuCl₄, t = 24 h, (b) 10 mM HAuCl₄, t = 48 h, (c) 100 mM APS, t = 12 h, and (d) 100 mM FeCl₃, t = 12 h.

increased to about 75 nm (Figure 3b). This time-dependent "hardening" of the OANI shell cannot be explained by any inhomogeneity present in the shell prior to the HAuCl₄ treatment. Moreover, the continued oxidation confirmed that the amount of HAuCl₄ present in the system was in excess. The fact that the excess HAuCl₄ was not able to completely oxidize the OANI shell indicates the slow diffusion of the ions. If the diffusion of HAuCl₄ were efficient, then it should have permeated the entire shell, and the concurrent oxidation throughout the shell would have given a uniformly "hardened" polymer. In fact, the clean edge of the "hardened" PANI layer in Figure 1g suggests that the rate of oxidation is much faster than the rate of diffusion. Similar rates would have caused a continuous gradient in the extent of oxidation and, thus, a smeared interface.

To further confirm the diffusion-limited oxidation process, we sought to modulate the permeability of the shell by swelling it with a small amount of organic solvent. The Au@OANI NPs

were incubated with 10 mM $HAuCl_4$ in H_2O/DMF mixture (95:5, v/v; DMF = N,N-dimethylformamide), followed by the same purifying and etching procedures. The extent of oxidation was obviously larger than the case above: Hardened shells of 50 nm were obtained after only 3 h, and 12 h incubation led to the hardening of entire shells (130 nm).[31] Other organic solvents, such as acetonitrile, acetone, and THF have similar effects in facilitating the diffusion of $HAuCl_4$.[31] It appeared that even small amounts of organic solvents can swell the hydrophobic OANI shells; the inserted solvent molecules opened up gaps among the oligomer chains[4] and facilitated ionic diffusion through them.

To understand if the slow diffusion was unique to $HAuCl_4$, we replaced it using other oxidants, such as $FeCl_3$ and ammonium persulfate (APS). The former is a cationic oxidant, whereas the later is anionic and insensitive to ligand coordination. Their slow diffusion was observed in both cases. When the same concentration of the oxidants was used (10 mM), the OANI shell was not hardened, and only bare AuNPs were recovered after the 2-propanol treatment. When the concentration was increased to 100 mM, partially hardened polymer shells of about 5 nm were obtained after 12 h (Figure 3c,d). Surprisingly, the shells appeared to be quite rigid without dents even though they were only 5 nm in thickness. Following the same arguments as above, the partial oxidation and the formation of sharp boundary indicated slower diffusion of the oxidants than their reactions. The need for higher concentrations can be explained by either that the high concentration makes the oxidants more reactive or that the high concentration leads to faster diffusion. Because the reduction potentials of the Fe^{3+}/Fe^{2+} ($E^0 = 0.77$ V) and $S_2O_8^{2-}/SO_4^{2-}$ ($E^0 = 2.01$ V) pairs were greatly different, it is unlikely that the 10 times increase in reactant concentration will significantly alter the thermodynamics of the redox chemistry. Most likely, the higher concentrations were needed for these two oxidants to compensate for their slower diffusion. Higher charges of these oxidative ions than $AuCl_4^-$ probably make them more difficult to diffuse through the polymer domains.[5,36] Interestingly, even with a large excess of oxidants (100 mM) and incubation for 5 days, the "hardened" shell did not increase significantly (remained about 5 nm).[31]

However, after being treated by 2-propanol, the polymer shell appeared to have improved permeability for neutral OANI as well as ionic species. It is expected that the diffusion of neutral OANI in the 2-propanol-swollen shell should be easier than the ionic diffusion through unswollen PANI in water. Nevertheless, the initial removal of the unreacted OANI was a slow process: When the $HAuCl_4$-treated Au@OANI NPs were incubated in 2-propanol for 20 min (as opposed to the 2 h incubation for those in Figure 1g), the inner section of OANI shell was not completely removed (Figure 4a). Loose polymer fibers were found extending the internal void (similarly for Figure 3b), whereas the hardened layer was already clearly visible. These hollow polymer shells appeared to be rigid with few deformations on their surface. In comparison, in Figure 1g the shells were often deformed. Further increase of the incubation time to 12 h did not cause noticeable change in the thickness of the "hardened" shell, except that more dents were formed (Figure 4b). The continuous weakening ("softening") of the shell suggested that even this "hardened" PANI layer was losing materials during the prolonged dissolving process, making it more porous.
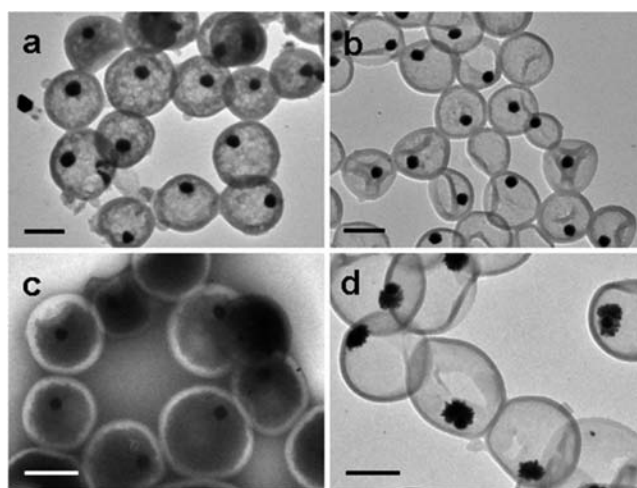

Figure 4. TEM images of the Au@PANI yolk-shell NPs obtained by etching the oxidized Au@OANI NPs in 2-propanol: (a) t = 20 min and (b) t = 12 h. Images of (c) Au@PANI yolk-shell NPs with negative stain applied during the drying of sample solution, showing the infiltration of the ionic stain, and (d) the NPs after growing dendritic branches on the Au cores of the Au@PANI yolk-shell NPs. Scale bars: 200 nm.

The solvent used here, 2-propanol, is not unique to this process; other polar organic solvents, such as ethanol, acetone, and 1,4-dioxane, could also be used to selectively dissolve the unreacted OANI section.[31] Thus, the removal of the OANI was not dependent on the reactivity of the solvents. It was likely a physical dissolving process rather than a reaction-based chemical etching process.

Ionic permeability of the PANI shells was also improved after "softening" by 2-propanol. When the Au@PANI yolk-shell NPs were mixed with an aqueous solution of an ionic stain, $(NH_4)_6Mo_7O_{24}$, and the mixture was dried on a TEM grid (on the order of several minutes), the negative stain was clearly observed inside the polymer shells (Figure 4c). To further confirm the improved ionic permeability, we tried to grow Au on the inner Au cores: After the Au@PANI yolk-shell NPs were incubated in aqueous $HAuCl_4$ solution for 15 min, the NPs were isolated by centrifugation and treated with aqueous aniline. Previously, it was known that aniline can reduce $HAuCl_4$ and cause Au branches to form on Au seeds.[37] Our observation of spiky Au core after the reaction (Figure 4d) confirmed the diffusion of both aniline and $HAuCl_4$ through the "softened" PANI shells.

Nature of the "Hardened" Shell. It is of importance to understand the nature of the "hardening" caused by $HAuCl_4$ treatment. It is known that the solubility of PANI depends on several factors. In general, larger molecular weight, higher oxidation state, and higher degree of acid doping lead to lower solubility in organic solvents.[29,38] The initially formed OANI can be completely dissolved in 2-propanol or THF: After incubating Au@OANI in the solvent for 1 h, only bare AuNPs were obtained after centrifugation.[31] After $HAuCl_4$ treatment, the polymer became insoluble in 2-propanol, but even this "hardened" shell can still be disintegrated in THF: After the Au@PANI yolk-shell NPs were incubated in THF for 6 h, the product isolated by centrifugation showed not only AuNPs but also insoluble polymer residue with irregular shape.[31] The supernatant contained low molecular weight polymer ($M_w = 910$). Its weight was estimated to be about 26 wt % of the

polymer in the Au@PANI yolk shell NPs; in comparison, the soluble polymer in the Au@OANI was over 95 wt % with M_w = 480.

The formation of insoluble PANI could be caused by several possible reasons. In a control experiment, a same concentration of HCl (10 mM) was used to replace $HAuCl_4$ in treating the Au@OANI; the resulting polymer shell could be easily removed by 2-propanol.[31] Hence, acid was not the main cause for the "hardening". On the other hand, it was possible that the $Au^{3+/+}$ ions or small AuNPs may bind to multiple OANI chains, cross-linking them and causing lower solubility. To investigate this possibility, the Au@PANI yolk-shell NPs were purified and then incubated with NaCN in pH = 8 solution for 12 h. Both the central 40 nm AuNP and the peripheral 5 nm AuNPs were removed by etching. The resulting hollow polymer NPs were insoluble in 2-propanol,[31] indicating that the coordination of OANI to Au did not play a major role in polymer solubility.

Because the thickness of the "hardened" PANI section increased with time, we believe that oxidation was the main cause for the solubility change. The oxidation of OANI could lengthen and/or cross-link the polymer chains, in addition to converting amine to imine groups. It is known that PANI can be oxidized to three different states: "leucoemeraldine", "emeraldine", and "pernigraniline", which have different ratios of amine to imine groups.[39] Typically, oxidation by weak oxidants in neutral pH condition gives oligomers that are rich in amine groups,[26,27] capable of being oxidized further. After being treated with an acidic and stronger oxidant, $HAuCl_4$, the amine groups of OANI are oxidized to imine groups and form PANI in "pernigraniline" state.[32,40]

IR was used to characterize the "hardened" shell. In comparison to the spectrum of the Au@OANI core−shell NPs, the peaks at 692 and 752 cm^{-1} diminished in the yolk-shell NPs (Figure 1d, line 2), suggesting an increase in the length of the polymer chains.[29] In the literature, the OANI/PANI peaks at ~1560−1590 and ~1480−1500 cm^{-1} were assigned to the C=C stretching of quinoid and benzenoid rings, respectively.[30] The quinoid moiety, along with its characteristic IR peak, could disappear when their imine groups were reduced to amine or when the quinoid rings were converted to benzenoid rings by cross-linking via the N atoms.[40,41] After $HAuCl_4$ treatment, the 1582 cm^{-1} peak significantly decreased relative to the 1493 cm^{-1} one. Because our reaction was carried out under an oxidative environment, most likely the OANI was cross-linked via the N atoms during its oxidation. Such cross-linking led to higher molecular weight and, thus, decreased solubility.

Estimation of the Diffusion Coefficient. Upon contacting $HAuCl_4$, OANI was protonated and oxidized to PANI. Then, the infiltrated oxidant has to penetrate two types of polymer layers. With ongoing reaction, the oxidized PANI layer gradually increases in thickness; the new reaction front progressively moves inside the polymer shell. If the diffusion through the oxidized PANI layer is the rate-determining step, it is expected that the rate of "hardening" should decrease due to the reduced amount of infiltrated oxidant. On the other hand, if the diffusion into the surface of the unreacted OANI layer is the rate-determining step, it is expected that the rate of "hardening" should remain roughly constant even with increasing shell thickness. The faster step of these two sequential processes should be insignificant to the reaction outcome. Comparing Figures 3b to 1f, the 8 times in the reaction time only led to

3.75 times in the thickness of the oxidized layer. Perhaps the most telling evidence was when APS or $FeCl_3$ was used as oxidant. In their large excess, prolonged incubation time (from 12 h to 5 days) did not lead to significant increase in the shell thickness (remained at about 5 nm). If the diffusion through the oxidized PANI was efficient (i.e., not the rate-determining step), then the reaction front should have moved through the OANI domain with roughly the same rate. Hence, we conclude that the diffusion through the PANI layer was the rate-determining step. The diffusion in OANI domain did not play an important role, simply because the oxidation only occurred at its shallow surface. In using $S_2O_8^{2-}$ and Fe^{3+} as oxidants, it is possible that their high ionic charges, the extensive cross-linking of the oxidized polymer, and the residue charged species (SO_4^{2-} and Fe^{2+}) could be responsible for stopping the ionic diffusion after hardening part of the shell.

If we assume that the diffusion of $AuCl_4^-$ in the "hardened" PANI layer is the rate-determining step, then we can estimate its rate. The volume of the oxidized polymer can be measured to calculate the infiltrated $AuCl_4^-$. To obtain the most conservative estimate, we assume that the OANI shell is compact with the density of bulk material (1.3 g/cm^3; in reality, the shell should be partially swollen by solvent and consume less $HAuCl_4$). Moreover, we set the reaction to go directly from aniline to PANI to maximize $HAuCl_4$ consumption, making the aniline:$HAuCl_4$ ratio to be 3:2. Suppose D is the position-independent diffusion coefficient. The rate of diffusion should be proportional to the concentration gradient of the ions (C_0 − 0), which is the typical assumption made in the literature.[42] The infiltrated ions should also be proportional to the area of the diffusion interface ($4\pi R^2$; R is the radius of the spherical interface at time t) and inversely proportional to the thickness of the oxidized layer ($R_0 - R$; R_0 is the outer radius of the polymer sphere). In eq 1, the amount of infiltrated oxidant is equal to the amount of $HAuCl_4$ necessary to fully oxidize the polymer (set as aniline here). The amount of polymer units is estimated as ($\rho_{PANI} \times V_{PANI}$)/$M$, where ρ_{PANI} is the density of PANI (1.3 g/cm^3), V_{PANI} is its volume $4\pi(R_0^3 - R^3)/3$, and M is the molecular weight of each aniline unit (89.13 g/mol). Both R and V_{PANI} are variables of t.

$$\int_0^t \frac{DC_0}{R_0 - R} \cdot 4\pi R^2 dt = \frac{2}{3} \cdot \frac{\rho_{PANI} V_{PANI}}{M} \tag{1}$$

$$D = \frac{\rho_{PANI}}{3C_0 M} \frac{(R_0 - R)^2}{t} \tag{2}$$

Deriving from eq 1, the diffusion coefficient D can be expressed as eq 2 (see the detailed steps in the Supporting Information). On the basis of the shell thickness at 6, 24, and 48 h, D is estimated to be 0.9×10^{-13}, 1.4×10^{-13}, and 1.6×10^{-13} cm^2/s, with the average being 1.3×10^{-13} cm^2/s. Though this constant is slowly increasing with time, the greater increase in shell thickness and the decrease in $4\pi R^2$ cause the infiltrated ions to decrease. As discussed above, these rate values have been significantly overestimated. However, it is still about 7000 times slower than the diffusion rate of Cl^- in PANI membrane, which is typically on the order of 10^{-9} cm^2/s.[42−44] It is known that the size of ions is a factor in ionic diffusion, for example, the rate of ClO_4^- in PANI (10^{-10} cm^2/s)[44] is slower than that of Cl^-. If we take this 10 times decrease into account, our observed rate of $AuCl_4^-$ diffusion coefficient is still 700 times slower than the typical rates of ionic diffusion in PANI.

The same method can be applied to estimate the rates of ionic diffusion in the presence of organic solvents. Even in the presence of small amounts of DMF (3%, 5%, or 10% in aqueous solutions), the swelling of the polymer shells led to dramatically increased rates of diffusion. At $t = 6$ h, the thickness of the "hardened" layer was 50, 80, and 105 nm, respectively, which was significantly thicker than the 20 nm shells obtained in pure water. Figure 5 is a plot showing the
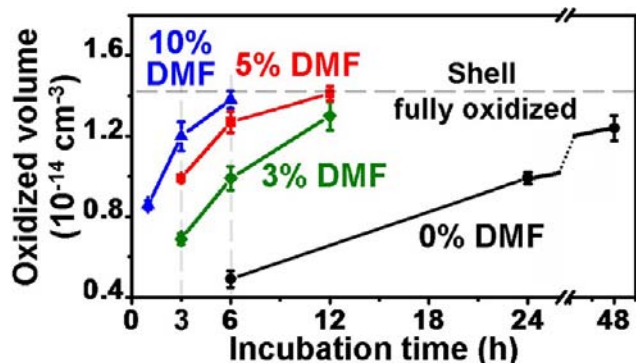

Figure 5. Effects of swelling on the ionic diffusion. A plot showing the volume of oxidized PANI against the incubation time.

oxidized volume of PANI (on the basis of the measured thickness)[31] against the incubation time in the HAuCl$_4$ solutions. Using eq 2, the averaged D was calculated to be 5.9×10^{-13}, 1.5×10^{-12}, and 2.3×10^{-12} cm^2/s for 3%, 5%, and 10% DMF solution, respectively. That is, the rates were 4, 11, and 17 times that of the rate in unswollen shells. This dramatic increase in ionic permeability upon swelling brings a perspective to the contributions that might result from micropores in typical polymer membranes.

It is generally very difficult to characterize pores in a membrane, in particular micropores. Pores can be formed by a variety of mechanisms. For example, when PANI is swollen by DMF or N-methyl-2-pyrrolidone (NMP), the solvent molecules are inserted among polymer chains. The subsequent loss of solvent by either evaporation or dissolution in water may leave behind micropores. On the other hand, large pores or cracks can form when a polymer membrane is subject to local mechanical stress during drying or fabrication. Typical methods for preparing polymer membrane involve casting or drying of polymers dissolved in organic solvents.[5,36] Though the resulting membranes often appear uniform, at the micrometer scale it is known that there exists dimples and grooves[36] that affect local uniformity in terms of thickness and density. This should be particularly problematic for polymers with poor solubility, for example, PANI formed using strong oxidants under acidic conditions.

In contrast, in our system the polymer shells were formed by in situ polymerization in the absence of organic solvent. Given their nanoscale shells, it is unlikely that they have been subject to significant mechanical stress. The subsequent oxidation reaction is critically dependent on the amount of infiltrated ions and, thus, is very sensitive to shell uniformity. We can rule out the presence of irregular pores in the OANI/PANI shells, because unless they are extremely uniform, we should not have obtained the "hardened" layer with nearly identical thickness. In general, the synthesis of nanoscale polymer shells is more reproducible and consistent among the individual particles. While we are also not able to directly characterize the

micropores in the polymer, the much slower rates of ionic diffusion can only be the result of fewer pores.

In traditional studies, it is hard to avoid inhomogeneity in large membranes. The measurement of overall penetrated ions masks the local differences in ionic permeability, so that a small number of pores might play a dominant role. In contrast, in nanoscale systems the shells are more uniform. If the infiltrated ions did cause local effects, they can be easily detected. Moreover, a thin shell means that pronounced effects can be induced by even a very small amount of infiltrated ions, or by minute changes in the shell, for example, when the polymer shell is swollen by only 3% DMF in water.

Our model system is simple because of the one-way diffusion of AuCl$_4^-$ ions and the fact that it is the rate-determining step in the overall process. In comparison, for example, the CN$^-$ etching of Au inside polymer shells involves the inward diffusion of both CN$^-$ and oxidant (O$_2$) as well as the outward diffusion of Au(CN)$_2^-$. In such a complex system, it is harder to distinguish the rate-determining step.

■ CONCLUSION

In summary, we demonstrate the feasibility of using a simple chemical reaction in nanoscale polymer shells to probe the rate of ionic diffusion. Our method is facile and sensitive. Such an unconventional model system could provide new perspectives that are complementary to the traditional studies. Our understanding in the diffusion process also allowed us unprecedented control in the synthetic design of organic/polymer shells. The partial oxidation and selective dissolving of such shells, in combination to the conversion of these shells to graphitic carbon, can enhance the synthetic tools for fabricating complex nanostructures in future nanodevices.

■ EXPERIMENTAL SECTION

Materials. Aniline (99%, Alfa Aesar) was distilled before use and stored at 4 °C. Hydrogen tetrachloroaurate(III) (99.9%, Au 49% on metals basis, Alfa Aesar), sodium citrate tribasic dihydrate (99.0%, Sigma), sodium dodecylsulfate (SDS, 99%, Alfa Aesar), aqueous H$_2$O$_2$ solution (35%, w/w, Alfa Aesar), FeCl$_3$ (98%, Alfa Aesar), and (NH$_4$)$_2$S$_2$O$_8$ (APS, 98%, Alfa Aesar) were used as received. Copper specimen grids (200 mesh) with Formvar/carbon support film were purchased from Beijing XXBR Technology Co. AuNPs (40 nm)[45] and gold nanorods (AuNRs)[46] were prepared following literature procedures. All solutions were prepared using ultrapure water (resistance > 18 MΩ cm^{-1}).

Characterization. TEM images were collected on a JEM-1400 (JEOL) operated at 100−120 kV. Fourier transform infrared (FT-IR) spectra were collected on a FT-IR spectrometer (Perkin-Elmer System 2000) using KBr pellets (32 scans), and the spectra were recorded with a resolution of 4 cm^{-1}. Raman spectra were recorded with a confocal Raman microscope (WiTec Alpha300) equipped with a piezo-scanner and 100× microscope objectives (NA = 0.9). Samples were excited with a He−Ne laser (488 nm, Coherent Inc.) with a spot size of ~1 μm. A GPC system consisting of an Agilent 1100 Series solvent delivery, sample injector, refractive index detector, and a 300 mm by 7.8 mm PLgel mixed-C, 5 μm column fitted with a guard column (Agilent Technologies, CA, USA) were used. THF at a flow rate of 1 mL/min was used, and 50 μL was injected per sample. EasiVial PS-M polystyrene standards (Agilent Technologies, CA, USA) were used for calibration. MALDI-ToF-MS analysis was performed on a Shimadzu Biotech AXIMA-TOF instrument.

Preparation of TEM Samples. TEM grids were treated with oxygen plasma in a Harrick plasma cleaner/sterilizer for 45 s to improve the surface hydrophilicity. The hydrophilic face of the TEM grid was then placed in contact with the sample solution. A filter paper

was used to wick off the excess solution on the TEM grid, which was then dried in air for 5 min.

In Figure 4c, $(NH_4)_6Mo_7O_{24}$ was used as the negative stain so that polymer shells appear white against the stained background. In this case, a sample solution was carefully mixed with stain solution on the surface of a plastic Petri dish ($[(NH_4)_6Mo_7O_{24}] = 4$ mM) and then placed in contact with the TEM grid.

Synthesis of Au@OANI Core−Shell NPs. Citrate-stabilized AuNP solution (~40 nm, 0.75 mL) was concentrated to a total of 10 μL by centrifugation at 6000 rpm (2900 g) for 8 min. After removal of supernatant, the isolated NPs were added to a mixture of aniline (0.13 mmol) and SDS (2.5 mM, 1.57 mL). Then the solution was vortexed for 5 s followed by addition of H_2O_2 (0.13 mmol). The total volume of the final mixture was 1.6 mL, where [aniline] = 81.2 mM, [SDS] = 2.5 mM, and $[H_2O_2]$ = 81.2 mM. After vortexing for 10 s, the reaction mixture was incubated at 75 °C for 12 h. To isolate the Au@ OANI core−shell NPs, the reaction mixture was centrifuged at 6000 rpm for 8 min, the supernatant was removed, and the concentrated NP solution was collected at the bottom of the Eppendorf tubes.

The Au@OANI core−shell NPs with thinner shells (average diameter: 110 nm) were prepared by use of a low concentration of aniline (27.1 mM) and H_2O_2 (27.1 mM) under otherwise identical conditions.

As-synthesized AuNRs (0.75 mL, d_{AuNR} = 22 nm, l_{AuNR} = 65 nm) were purified by first centrifuging at 7000 rpm (4000 g) for 10 min and then dispersing the concentrated AuNRs in water. This purification was repeated once more to further remove the excess CTAB. After these purification steps, the AuNRs were encapsulated by OANI using the standard method.

Synthesis of Au@PANI Yolk-Shell NPs. The as-synthesized Au@ OANI core−shell NP solution (0.5 mL) was concentrated by centrifugation (<10 μL) and then added into an aqueous $HAuCl_4$ solution (10 mM, 0.5 mL). The mixture was incubated at room temperature for 6−48 h on a shaker. After that, the solution was concentrated by centrifugation, and then the NPs were redispersed in 2-propanol (0.5 mL) for 2−12 h. At last, after centrifugation at 6000 rpm for 8 min, the Au@PANI yolk-shell NPs were collected and dispersed in water for further characterization.

In a different set of experiments, the purified Au@OANI core−shell NPs were treated with 10 mM aqueous $HAuCl_4$ solution containing different amounts of DMF (3%, 5%, and 10% in volume) for a specified time (1−12 h), followed by the same purifying and etching procedures. Different organic solvents including acetone, acetonitrile, and THF were also tested in place of DMF in the above experiment.

In additional sets of experiments, the purified Au@OANI core−shell NPs were incubated in aqueous $FeCl_3$ (0.1 M, 0.5 mL) or APS (0.1 M in 0.1 M HCl, 0.5 mL) solutions for a specified time (12−120 h), followed by the same purifying and etching procedures. Residue $FeCl_3$ can cause etching of the AuNPs. Typically, the product solution was purified multiple times to minimize such etching during the treatment in 2-propanol.

Etching of Au@PANI Yolk-Shell NPs. The isolated Au@PANI yolk-shell NPs (5 μL) were added to NaCN in pH = 8 solution, and the mixture was incubated for 12 h (50 mM, 3 μL). After purification, the isolated NPs were incubated in 2-propanol for 2 h. The residue supernatant and solution were treated with excess $FeCl_3$ to detoxify the CN^- ions by forming $[Fe(CN)_6]^{3-}$. (Caution: KCN is extremely poisonous even at low concentrations; it should be handled with great care. Never add any acid to KCN solutions.)

Preparation of Au@C Yolk-Shell NPs. The purified Au@PANI yolk-shell NPs were dried under vacuum and then put into a quartz tube in an electric furnace under Ar flow (0.2 L min^{-1}). The sample was heated up to 1000 °C for carbonization at a heating rate 3 °C min^{-1}, held for 3 h, and then naturally cooled to room temperature. After carbonization, the powder was directly used for Raman characterization. For TEM characterization, the NPs were dispersed in 30 μL water by sonication.

Growth of Dendritic Branches on the Au Cores of the Au@ PANI Yolk-Shell NPs. 0.5 mL of as-prepared Au@PANI yolk-shell NP solution was isolated and then dispersed in an aqueous $HAuCl_4$ solution (1 mM, 0.5 mL). The mixture was incubated at room temperature for 15 min. After that, the isolated NPs were added into an aqueous aniline solution (2 mM, 0.5 mL) and incubated at room temperature for 2 h to grow dendritic branches on the Au cores. At last, the mixture was centrifuged at 6000 rpm for 8 min, and the spiky Au@PANI yolk-shell NPs were collected for further characterization.

■ ASSOCIATED CONTENT

Ⓢ Supporting Information

Raman spectrum, MALDI-ToF-MS, and large-area supporting TEM figures. This material is available free of charge via the Internet at http://pubs.acs.org.

■ AUTHOR INFORMATION

Corresponding Author

hongyuchen@ntu.edu.sg

Notes

The authors declare no competing financial interest.

■ ACKNOWLEDGMENTS

■ REFERENCES

(1) Janata, J.; Josowicz, M. *Nat. Mater.* **2003**, *2*, 19.

(2) Nystrom, G.; Razaq, A.; Stromme, M.; Nyholm, L.; Mihranyan, A. *Nano Lett.* **2009**, *9*, 3635.

(3) Huang, J.; Virji, S.; Weiller, B. H.; Kaner, R. B. *Chem.—Eur. J.* **2004**, *10*, 1315.

(4) Virji, S.; Huang, J. X.; Kaner, R. B.; Weiller, B. H. *Nano Lett.* **2004**, *4*, 491.

(5) Deligoz, H. *J. Appl. Polym. Sci.* **2007**, *105*, 2640.

(6) Lou, X. W.; Archer, L. A.; Yang, Z. C. *Adv. Mater.* **2008**, *20*, 3987.

(7) Kamata, K.; Lu, Y.; Xia, Y. N. *J. Am. Chem. Soc.* **2003**, *125*, 2384.

(8) Lai, X. Y.; Li, J.; Korgel, B. A.; Dong, Z. H.; Li, Z. M.; Su, F. B.; Du, J. A.; Wang, D. *Angew. Chem., Int. Ed.* **2011**, *50*, 2738.

(9) Lee, J.; Park, J. C.; Song, H. *Adv. Mater.* **2008**, *20*, 1523.

(10) Arnal, P. M.; Comotti, M.; Schuth, F. *Angew. Chem., Int. Ed.* **2006**, *45*, 8224.

(11) Li, W.; Deng, Y. H.; Wu, Z. X.; Qian, X. F.; Yang, J. P.; Wang, Y.; Gu, D.; Zhang, F.; Tu, B.; Zhao, D. Y. *J. Am. Chem. Soc.* **2011**, *133*, 15830.

(12) Dong, Z. H.; Lai, X. Y.; Halpert, J. E.; Yang, N. L.; Yi, L. X.; Zhai, J.; Wang, D.; Tang, Z. Y.; Jiang, L. *Adv. Mater.* **2012**, *24*, 1046.

(13) Lai, X. Y.; Halpert, J. E.; Wang, D. *Energy Environ. Sci.* **2012**, *5*, 5604.

(14) Lu, Y.; Zhao, Y.; Yu, L.; Dong, L.; Shi, C.; Hu, M. J.; Xu, Y. J.; Wen, L. P.; Yu, S. H. *Adv. Mater.* **2010**, *22*, 1407.

(15) Xing, S. X.; Tan, L. H.; Chen, T.; Yang, Y. H.; Chen, H. Y. *Chem. Commun.* **2009**, 1653.

(16) Zhu, J. X.; Sun, T.; Hng, H. H.; Ma, J.; Boey, F. Y. C.; Lou, X. W.; Zhang, H.; Xue, C.; Chen, H. Y.; Yan, Q. Y. *Chem. Mater.* **2009**, *21*, 3848.

(17) Sun, Y. G.; Wiley, B.; Li, Z. Y.; Xia, Y. N. *J. Am. Chem. Soc.* **2004**, *126*, 9399.

(18) Yin, Y. D.; Rioux, R. M.; Erdonmez, C. K.; Hughes, S.; Somorjai, G. A.; Alivisatos, A. P. *Science* **2004**, *304*, 711.

(19) Zhang, T. R.; Ge, J. P.; Hu, Y. X.; Zhang, Q.; Aloni, S.; Yin, Y. D. *Angew. Chem., Int. Ed.* **2008**, *47*, 5806.

(20) Zhang, Q.; Zhang, T. R.; Ge, J. P.; Yin, Y. D. *Nano Lett.* **2008**, *8*, 2867.

(21) Roca, M.; Haes, A. J. *J. Am. Chem. Soc.* **2008**, *130*, 14273.

(22) Wong, Y. J.; Zhu, L. F.; Teo, W. S.; Tan, Y. W.; Yang, Y. H.; Wang, C.; Chen, H. Y. *J. Am. Chem. Soc.* **2011**, *133*, 11422.

(23) Niu, Z. W.; Yang, Z. H.; Hu, Z. B.; Lu, Y. F.; Han, C. C. *Adv. Funct. Mater.* **2003**, *13*, 949.

(24) Bai, M. Y.; Cheng, Y. J.; Wickline, S. A.; Xia, Y. N. *Small* **2009**, *5*, 1747.

(25) Sun, H.; He, J. T.; Xing, S. X.; Zhu, L. F.; Wong, Y. J.; Wang, Y. W.; Zhai, H. J.; Chen, H. Y. *Chem. Sci.* **2011**, *2*, 2109.

(26) Stejskal, J.; Sapurina, I.; Trchova, M.; Konyushenko, E. N. *Macromolecules* **2008**, *41*, 3530.

(27) Zhang, Y. S.; Xu, W. H.; Yao, W. T.; Yu, S. H. *J. Phys. Chem. C* **2009**, *113*, 8588.

(28) Xing, S. X.; Tan, L. H.; Yang, M. X.; Pan, M.; Lv, Y. B.; Tang, Q. H.; Yang, Y. H.; Chen, H. Y. *J. Mater. Chem.* **2009**, *19*, 3286.

(29) Laska, J.; Widlarz, J. *Polymer* **2005**, *46*, 1485.

(30) Feng, X. M.; Yang, G.; Xu, Q.; Hou, W. H.; Zhu, J. P. *Macromol. Rapid Commun.* **2006**, *27*, 31.

(31) See Supporting Information for details.

(32) Tseng, R. J.; Huang, J. X.; Ouyang, J.; Kaner, R. B.; Yang, Y. *Nano Lett.* **2005**, *5*, 1077.

(33) Yang, H. F.; Yan, Y.; Liu, Y.; Zhang, F. Q.; Zhang, R. Y.; Meng, Y.; Li, M.; Xie, S. H.; Tu, B.; Zhao, D. Y. *J. Phys. Chem. B* **2004**, *108*, 17320.

(34) Stankovich, S.; Dikin, D. A.; Piner, R. D.; Kohlhaas, K. A.; Kleinhammes, A.; Jia, Y.; Wu, Y.; Nguyen, S. T.; Ruoff, R. S. *Carbon* **2007**, *45*, 1558.

(35) Jang, J.; Li, X. L.; Oh, J. H. *Chem. Commun.* **2004**, 794.

(36) Wen, L.; Kocherginsky, N. M. *Synth. Met.* **1999**, *106*, 19.

(37) Pan, M.; Xing, S. X.; Sun, T.; Zhou, W. W.; Sindoro, M.; Teo, H. H.; Yan, Q. Y.; Chen, H. Y. *Chem. Commun.* **2010**, *46*, 7112.

(38) Abe, M.; Ohtani, A.; Umemoto, Y.; Akizuki, S.; Ezoe, M.; Higuchi, H.; Nakamoto, K.; Okuno, A.; Noda, Y. *J. Chem. Soc., Chem. Commun.* **1989**, 1736.

(39) Li, D.; Huang, J. X.; Kaner, R. B. *Acc. Chem. Res.* **2009**, *42*, 135.

(40) Hatchett, D. W.; Josowicz, M.; Janata, J.; Baer, D. R. *Chem. Mater.* **1999**, *11*, 2989.

(41) Strong, V.; Wang, Y.; Patatanyan, A.; Whitten, P. G.; Spinks, G. M.; Wallace, G. G.; Kaner, R. B. *Nano Lett.* **2011**, *11*, 3128.

(42) Kocherginsky, N. M.; Lei, W.; Wang, Z. *J. Phys. Chem. A* **2005**, *109*, 4010.

(43) Treptow, F.; Jungbauer, A.; Hellgardt, K. *J. Membr. Sci.* **2006**, *270*, 115.

(44) Foot, P. J. S.; Simon, R. *J. Phys. D: Appl. Phys.* **1989**, *22*, 1598.

(45) Frens, G. *Nat. Phys. Sci.* **1973**, *241*, 20.

(46) Nikoobakht, B.; El-Sayed, M. A. *Chem. Mater.* **2003**, *15*, 1957.